JOURNAL OF CATALYSIS 16, 117–125 (1970)

# The Oxidation of Ethylene over Evaporated Palladium–Rhodium Alloy Films

## I. Film Structure with Special Reference to Phase-Separation

R. L. MOSS, H. R. GIBBENS, AND D. H. THOMAS

*From the Warren Spring Laboratory, Stevenage, England*

Received May 28, 1969

Recent thermodynamic data for Pd–Rh alloys confirm earlier experimental observations that annealing for very prolonged periods below 850°C causes separation into two FCC phases over a wide composition range. Palladium–rhodium alloy films, prepared by slow simultaneous evaporation of the component metals on to a glass substrate at 400°C, show good bulk homogeneity (expected lattice constants, symmetrical X-ray diffraction profiles) at the ends of the composition range (0–30 and 80–100% Rh) but tend to phase-separation at intermediate compositions. After use as catalysts for ethylene oxidation, Pd–Rh alloy films with 30–80% Rh show clear evidence of two "phases" contributing to the diffraction profile; Phase I varied in composition and was deficient in Rh compared with the corresponding solid solution and Phase II had a composition of 88 ± 5% Rh in accord with the solubility diagram. Palladium-rich films showed strong (111) preferred orientation, weakening with increasing Rh content so that the crystallites in almost pure Rh films had approximately random orientation.

The formation of Pd–Rh alloy films is considered with regard to the interpretation of the catalytic results according to composition: *0–30% Rh;* diffusion during film formation and use is limited and inhibits the phase-separation indicated, giving a homogeneous alloy. Evidence was found for hydrogen solubility in alloy films with <10% Rh after carrying out ethylene oxidation with partial consumption of the reactants, indicating a subdivision of this composition range. (Films with up to ~30% Rh could be charged with hydrogen if all the oxygen was consumed, leaving unreacted ethylene.) *40–80% Rh;* a mechanism is proposed involving the preferential nucleation of Rh whereby Phase II can form in conditions of limited diffusion as a Rh-rich kernel to the crystallite, surrounded by a Rh-deficient solid solution of variable composition. *80–100% Rh;* the process continues but the "phases" are sufficiently close in composition to remain undetected.

### INTRODUCTION

If the catalytic activity of the noble metals is generally related to their electronic properties, then it seems reasonable to expect that some of their alloys might possess the properties required for optimum activity. There has been recent interest in the binary alloys of Ru, Rh, Pd, Pt, etc., for $CH_4$–$D_2$ exchange (*1–3*), propane cracking (*3*), methanol decomposition (*4*) and the isomerization of pentane (*5*). In liquid-phase hydrogenations, "synergistic" effects have been reported (*6*) and peaks in activity have been observed in a series of reduced (mixed) oxide catalysts (*7, 8*) and with supported Pt–Rh alloys (*9, 10*).

Now, it has been shown, using evaporated alloy films of Group VIII and IB metals, that various complications arise which obscure the pattern of activity expected from the bulk electronic properties of the system. Phase-separation was found in Cu–Ni alloys (*11, 12*) and silver-enrichment at the surface of Pd–Ag alloy films during ethylene oxidation was suspected (*13, 14*). There are indications that some of the

alloys formed from pairs of Group VIII metals may also tend to phase-separation, which may develop first at the catalyst surface and confuse the interpretation of results. Therefore it seems helpful to prepare such alloy catalysts in the form of evaporated films where surface diffusion during alloy formation, and thus the rate of equilibration is enhanced and where physical methods of examination are more informative about the catalyst structure. Convenient techniques have been worked out for the preparation of alloy films with a uniform composition over an extended area and for the detailed examination of their structure (*13*, *15*). The particular choice of the Pd–Rh system and the ethylene oxidation reaction is discussed in the Introduction to Ref. (*16*).

## Experimental Methods

References (*13*) and (*15*) provide detailed accounts of alloy film preparation and examination and only a general outline is given below, noting some features particular to the present work. Alloy films were formed on the inner surface of spherical Pyrex glass reaction vessels (held at 400°C) by slow simultaneous evaporation from short concentric spirals of 0.5 mm diameter Pd and Rh wire (Johnson, Matthey and Co. Ltd., "spectrographically standardized") and then annealed for 1 hr at the same temperature. The reaction vessel was sealed directly to a glass vacuum-system incorporating greaseless stopcocks; the vessel and parts of the system were baked above 450°C and vacuum of $10^{-6}$ torr (1 torr = 133.32 N/m$^2$) measured with an ionization gauge were usual. Before depositing a film, the Pd and Rh spirals were outgassed for ~1 hr at temperatures close to the evaporation points of the metals while the glassware was continuously evacuated and heated.

At the end of each catalytic experiment, the composition of the alloy film at 12 representative parts of the reaction vessel was determined by X-ray fluorescence analysis. For alloy films containing <5% Rh, it was necessary to use the $L\alpha$ emissions, otherwise the composition was determined from the intensities of the Pd$K\alpha$ and Rh$K\alpha$. With attention to the positioning of the spirals, Pd–Rh alloy films showed the same uniformity of composition over the 220-cm$^2$ area of the reaction vessel observed previously for Pd–Ag alloy films (*13*). The total weight of catalyst (film) involved in each experiment was found from the combined weight loss from the two spirals.

Specimens for X-ray diffraction or electron microscopy were obtained by stripping the film from fragments of the reaction vessel. An edge of the film was detached from the glass by dipping in 10% HF solu-

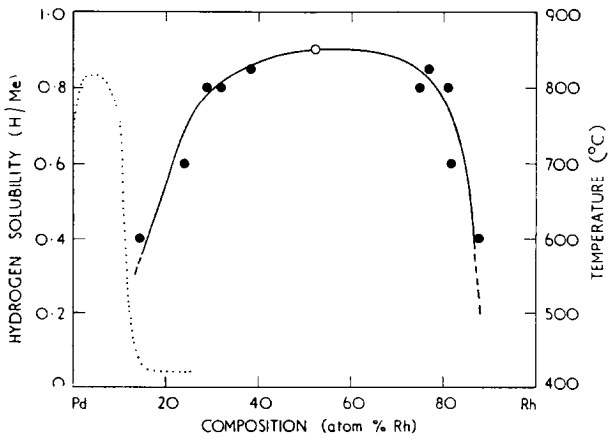


FIG. 1. Limits of the miscibility gap in Pd–Rh alloys calculated from the lattice constants of the two-phase alloys between 600 and 825°C [Ref. (*17*)] (—); Hydrogen solubility at 760 torr as a function of Rh content [Ref. (*19*)] (· · ·).

TABLE 1
THERMODYNAMIC PROPERTIES OF Pd–Rh ALLOYS AT 1575°K

| Composition (at. % Rh) | (cal/g-atom) $\Delta\bar{G}$ | (cal/g-atom) $\Delta\bar{H}$ | (cal/g-atom deg) $\Delta\bar{S}$ |
|---|---|---|---|
| 10 | −570 | 1210 | 1.13 |
| 20 | −800 | 1880 | 1.70 |
| 30 | −920 | 2050 | 1.89 |
| 40 | −950 | 2310 | 2.07 |
| 50 | −950 | 2410 | 2.13 |
| 60 | −940 | 2290 | 2.05 |
| 70 | −880 | 2030 | 1.85 |
| 80 | −770 | 1520 | 1.46 |
| 90 | −570 | 790 | 0.86 |

tion, then the film floated off in distilled water; the detached film was collected on either a thin square of glass or on an electron microscope sample grid.

## RESULTS AND DISCUSSION

### *Solubility Limits*

Raub (*17*) gives lattice constants for Pd–Rh alloys, quenched from 1300°C, which vary smoothly with composition and show only a small positive deviation from Vegard's law. Cooling slowly over 14 days gave the same results, but prolonged periods of vacuum annealing below 850°C revealed the existence of a wide miscibility gap. The establishment of equilibrium was extremely slow with these arc-melted specimens and at 600°C (after 196 days) only the 50–50 alloy separated into the two face-centered cubic phases. Figure 1 shows the limits of the miscibility gap calculated from the lattice constants of the two-phase alloys between 825 and 600°C.

Recently, the thermodynamic properties of Pd–Rh alloys at ~1300°C were derived from vapor pressure data (*18*) and confirm the tendency to phase-separation. The enthalpies of formation are endothermic (Table 1) and only temperatures above ~860°C produce a sufficiently large $T\Delta S$ term to yield negative values of $\Delta G$ (assuming the temperature-independence of $\Delta H$ and $\Delta S$), at compositions between 10 and 90% Rh, in accord with the above experimental observations. Similarly, a wide miscibility gap is indicated for the alloy preparation temperature, 400°C, used in the present work.

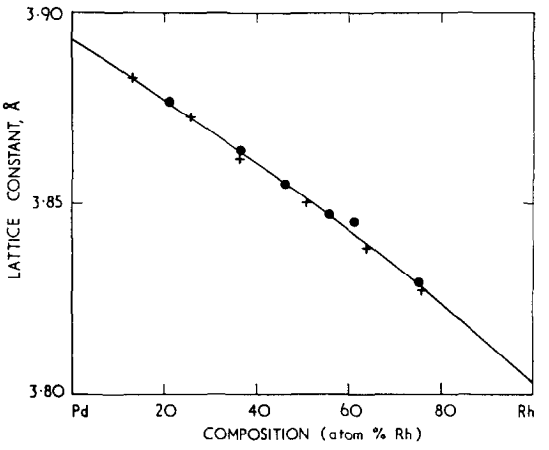


FIG. 2. Lattice constants for evaporated Pd–Rh alloy films, deposited and annealed at 400°C, unused in catalytic reaction, ●; lattice constants (converted from $kX$ units) from Ref. (*17*), obtained with arc-melted quenched specimens, +.

### *Structure of Unused Alloy Films*

In view of the evidence presented above, which showed clearly the miscibility gap existing in bulk Pd–Rh alloys, it was of interest to examine how far films, prepared by slow simultaneous evaporation of the component metals and annealed at 400°C, exhibited this behavior.

Figure 2 records lattice constants for Pd–Rh alloy films, unused in catalytic reaction, calculated from the centroid of individual X-ray profiles and extrapolated to $\theta = 90°$ using the Nelson-Riley function. For comparison, the lattice constants (converted from $kX$ units) obtained by Raub (*17*) using arc-melted quenched Pd–Rh alloys are also shown. The close agreement between the present results for alloy films and Raub's results is useful evidence for the internal consistency of the present X-ray fluorescence and X-ray diffraction results and for the absence of gross inhomogeneity.

It is believed, however, that the symmetry of the diffraction profile, obtained with a counter-diffractometer, is a more sensitive indication of a tendency to phase-separation. Figure 3 (left-hand column)

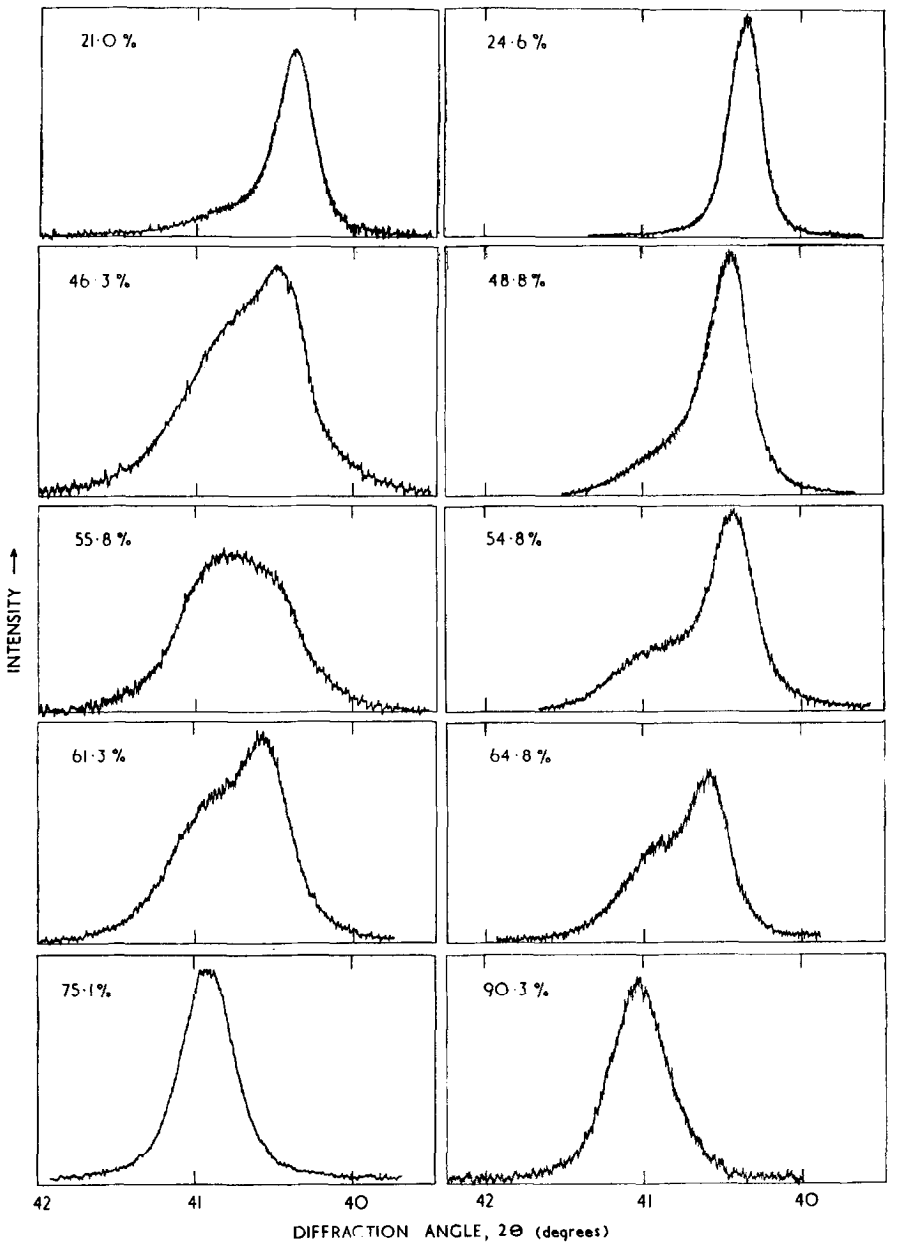


FIG. 3. The X-ray diffraction profiles from (111) planes: (left-hand column), Pd–Rh films not used in catalytic reaction; (right-hand column), after use as catalysts for $C_2H_4$ oxidation; compositions in at. % Rh

shows a selection of (111) diffraction profiles for separate alloy films of different composition which had not been used in catalytic reaction. Alloy films with less than ~40% Rh yielded reasonably symmetrical diffraction profiles although the 21.0% Rh film showed some "tailing" on the high-angle side and the 36.3% Rh film (not shown) has increased profile width. Beyond this Rh content, the profiles showed evidence of inhomogeneity, perhaps due to phase-separation. The profile for the 55.8% Rh film, while not assymmetrical like the 46.3 and 61.3% Rh films, is clearly misshapen compared with the standard diffraction profile. The (222) diffraction profile

for the 61.3% Rh film, not shown in Fig. 3, split into a doublet (other than the $\alpha_1 - \alpha_2$ separation) corresponding to phases with 43 and 82% Rh. Eventually at higher Rh contents (75.1% Rh), perfectly symmetrical diffraction profiles were again found.

It is concluded that alloy films with apparently good bulk homogeneity were formed at either end of the composition range. The extent of solubility is somewhat greater than the information provided in the previous section would indicate. However, over a wide range of intermediate compositions, there is evidence of a tendency to phase-separation.

*Alloy Films after Catalytic Reaction*

As an essential requirement for interpreting the variation in catalytic activity for ethylene oxidation as a function of alloy composition (*16*) the structure of the films after catalytic reaction was examined by X-ray diffraction. In general, each film had been used at ~150–200°C with a single reaction mixture, then sometimes heated overnight in 50 torr of $H_2$ at 240°C, evacuated at this temperature and a second reactant mixture admitted. A selection of X-ray diffraction profiles obtained from these films is shown in Fig. 3 (right-hand column).

The X-ray diffraction profiles from films with less than 10% Rh were approximately symmetrical but consistently showed "tailing" towards the low-angle side; above this composition up to 25% Rh, the profiles were perfectly symmetrical. The (111) profile for a 24.6% Rh film is shown in Fig. 3, but inspection of the (222) profile, after $\alpha_1 - \alpha_2$ resolution, showed no evidence of phase-separation. Even at 45.3% Rh, although the profile shows marked asymmetry, a separation into two peaks could not be identified. However, a much heavier film with 48.8% Rh, again showing asymmetry in the (111) profile, Fig. 3, gave rise to a (222) profile in which two peaks could be discerned, and from one of these a value for the lattice constant was calculated.

At higher Rh contents, above ~50% up to ~80% Rh, the occurrence of two peaks in each diffraction profile was apparent and easily recognized in the higher-angle reflections where these are present. At still higher Rh contents (cf. 90.3% Rh film in Fig. 3), the profiles are again symmetrical. Thus, the pattern of solubility at either end of the composition range, with a tendency to phase-separation at intermediate compositions observed with unused films, is also clearly evident for films used in ethylene oxidation.

**Lattice constants.** Lattice constants observed for many of the Pd–Rh alloy films

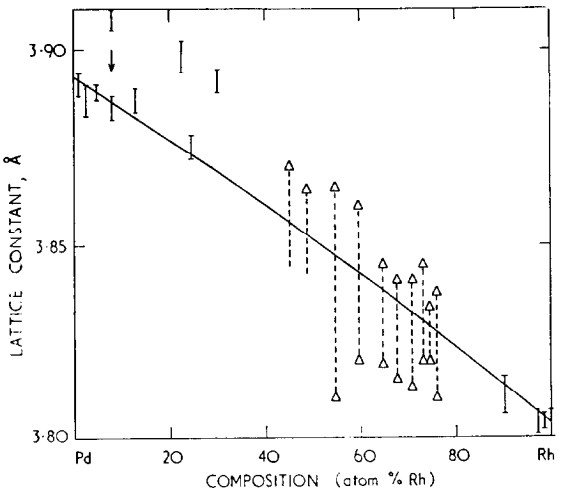


FIG. 4. Lattice constants for Pd–Rh alloy films used to catalyze $C_2H_4$ oxidation: films where phase-separation is not apparent, vertical bar; positions of two peaks in diffraction profile, triangles joined by vertical broken line.

used to catalyze ethylene oxidation are shown in Fig. 4. Where phase-separation has not yet developed, the lattice constant is shown by a vertical bar. Values of $a_0$ were again calculated from the positions of the centroids of individual diffraction profiles extrapolated to $\theta = 90°$ and the length of the vertical bar indicates the uncertainty. Where the diffraction profiles showed evidence of phase-separation, then lattice constants were calculated using the positions of the two peaks in the profile. These results are shown in Fig. 4 by two open triangles joined by a vertical broken line. Near the middle of the composition range, the position of only one of these peaks could be identified although the diffraction profiles were markedly asymmetrical. The expected value of the lattice constant for a given composition obtained from Fig. 2 is also shown.

The lattice constants of alloys with low and high Rh contents, occur at the expected value with the exceptions which are discussed below. It is convenient to describe the maxima in the profiles for alloys with intermediate compositions as arising from two "phases," (I) and (II). The upper set of lattice constants from Phase I decreased steadily with increasing Rh content. The lower set of lattice constants from Phase II showed no clear trend with composition and had a mean value of 3.816 Å corresponding to a composition of 88 at. % Rh with a variation of ±5%. Figure 1 shows that the curve indicating the limits of the miscibility gap falls steeply at the Rh-rich side and that, for an alloy preparation temperature of 400°C, an equilibrium composition of 88 ± 5% Rh for Phase II is not unreasonable.

**Hydrogen solubility.** Figure 1 also shows isobaric solubilities at 760 torr of $H_2$ as a function of Rh content (*19*). At compositions beyond ~20% Rh, the hydrogen solubility is extremely limited, but alloys with less than 10% Rh dissolve more hydrogen than Pd itself. Data in Refs. (*20*) and (*21*) suggest that the hydrogen solubility limit occurs at about 30% Rh.

The anomalously high lattice constants for films with 8.0, 22.6, and 30.1% Rh (Fig. 4) associated with assymmetrical diffraction profiles, are believed to be due to dissolved hydrogen. In a typical experiment, the same gas mixture was used at three temperatures and up to 60–80% of the oxygen was consumed, whereas over these Pd–Rh films, the oxygen consumption was 100%. When a sample of the 8% Rh film was subsequently heated in vacuum for 50 hr at 400°C and again examined by X-ray diffraction, then the expected lattice constant was found *and the diffraction profile*

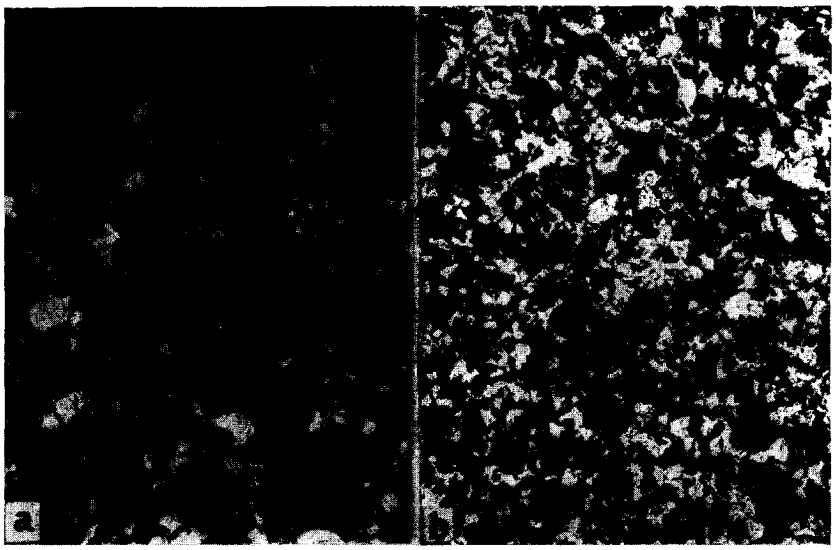


FIG. 5. Electron micrographs of Pd–Rh alloy films, magnification 20,000×; (a) 2.5% Rh, 19.7 mg; (b) 59.7% Rh, 21.0 mg.

*had become symmetrical.* The lattice constant of the film with 30.1% Rh could also be reduced by degassing to exactly the correct value. The excess hydrogen content of the system (contained in $C_2H_4$) after total oxygen consumption is sufficient to charge up the small volume of the alloy film.

Therefore it would seem that the "tailing" of the diffraction profiles from other used alloy films with less than 10% Rh is also caused by some hydrogen dissolution. The tailing occurs on the low-angle side, i.e., corresponding to material with a higher lattice constant than the bulk of the alloy specimen, and is consistent with the expansion of the lattice by hydrogen.

**Crystallite size and orientation.** Electron micrographs of Pd–Rh alloy films of widely different Rh content but similar weights are shown in Fig. 5. Both films are polycrystalline and not extensively sintered, unlike Pd–Ag films with high Ag contents (*13*) prepared by the same technique. The crystallite size decreases to some extent with increasing Rh content.

The areas under the diffraction profiles were measured for films of varying composition but again with similar weights (Table 2). These areas have been corrected for changes in the X-irradiated area by dividing each by ($\sin \theta_{111}/\sin \theta_{hkl}$) and are directly related to the volume of alloy in the $\{hkl\}$ orientation, but only reflecting planes parallel to the glass substrate contribute to the X-ray intensity. Data from the ASTM Index for random powder samples of Pd and Rh are also included in Table 2. The occurrence of preferred orientation in most of the alloy films is apparent, i.e., a strong {111} texture has developed. Only as the Rh content increases does this preference weaken so that an almost pure Rh film shows nearly random orientation.

**Model structure for Pd–Rh alloy films.** In the vapor phase the component metal atoms suffer no miscibility restriction and, if the substrate was sufficiently cold, would condense near the point of impingement to produce a homogenous solid solution although the equilibrium phase-diagram indicates a miscibility gap. By this means the range of mutual solubility of Pd and Rh might be extended. However, under reaction conditions at higher temperatures, the outermost layers of the crystallites, at least, might undergo phase-separation. This would be a severe complication and so conditions were chosen to produce a more stable film structure. The construction of these Pd–Rh alloy films, composed of two phases over a wide composition range, is considered below.

A process of continuous nucleation is envisaged on a substrate which initially is the glass wall of the reaction vessel but subsequently, and for the most of the film deposition time, is the film material itself. The crystallites formed sinter together during film deposition and during the short period of annealing at the same substrate temperature (400°C). Most observations relating to heterogeneous nucleation are

TABLE 2
CRYSTALLITE ORIENTATION

| Composition (at. % Rh) | Film wt. (mg) | Corrected X-ray intensities | | | | |
|---|---|---|---|---|---|---|
| | | (111) | (200) | (220) | (311) | (222) |
| 1.09 | 26.85 | 100 | 0.2 | <0.1 | 0.1 | 9 |
| 4.85 | 27.20 | 100 | 5 | 1 | 2 | 6 |
| 12.9 | 30.50 | 100 | 0.6 | <0.1 | 0.4 | 11 |
| 24.6 | 25.30 | 100 | 3 | 0.3 | 2 | 11 |
| 54.8 | 27.65 | 100 | 13 | 3 | 9 | 10 |
| 76.1 | 26.00 | 100 | 8 | 1 | 3 | 4 |
| 97.2 | 29.25 | 100 | 39 | 25 | 25 | 6 |
| Pd powder (ASTM) | | 100 | 42 | 25 | 24 | 8 |
| Rh powder (ASTM) | | 100 | 50 | 26 | 33 | 11 |

consistent with the general theory which assumes metastable equilibrium between single adatoms and polyatomic aggregates on the substrate surface to which macroscopic thermodynamic properties are ascribed (*22*), although perhaps not entirely justified for small aggregates.

There is a point at which these aggregates reach a critical size of minimum stability, $r^*$, and the free energy of formation $\Delta G^*$ is a maximum. Further addition of material to the critical nucleus decreases the free energy and produces a stable growing nucleus. The nucleation rate is the product of the concentration of critical nuclei $N^*$ given by:

$$N^* = N_{ad} \exp(-\Delta G^*/kT), \qquad (1)$$

and the rate at which adsorbed atoms migrate and become incorporated into the nuclei, where $N_{ad}$ is the adatom concentration on the substrate. The free energy of formation of an aggregate is expressed as the sum of terms including surface free energies and $\Delta G_v$, the free energy difference between supersaturated vapor of pressure $p$ and condensate of equilibrium vapor pressure $p_e$ and atomic volume $\Omega$ where

$$\Delta G_v = -(kT/\Omega) \ln(p/p_e). \qquad (2)$$

The nucleation rate is strongly dependent on the $\Delta G_v$ term in $\Delta G^*$ and, for any one deposition rate, the supersaturation ratio at the substrate temperature $T$ is given principally by the bulk heat of sublimation. The respective values for Pd and Rh are 89 and 133 kcal/g and therefore Rh should form more nuclei than Pd on a glass substrate which has a weak affinity for the film material. The interfacial (aggregate–substrate) free energy and substrate surface energy terms in $\Delta G^*$ are more important for nucleation on a metal substrate. After the initial deposition on glass, condensation indeed occurs on the film material itself and there might not be an effective nucleation barrier for either metal ($r^* < 2$ atoms) during much of the film formation process but for the high substrate temperature (400°C).

It is proposed that Pd–Rh alloy films are formed under the conditions used, as follows:

**Composition range 0–30% Rh.** In the presence of an excess Pd flux, any tendency for Rh to nucleate preferentially is nullified, and apparently insufficient diffusion occurs during annealing or under reaction conditions to effect the formation of separate phases. The resistance of bulk Pd–Rh specimens to phase-separation is well established (*17*).

**Composition range 30–80% Rh.** Because of the logarithmic dependence of $\Delta G_v$ on $p$ in Eq. (2) and therefore on the impingement rate, a modest decrease in the Rh flux relative to the Pd flux should not affect its preferential nucleation, if this occurs for the reasons discussed above. It is proposed that beyond 40% Rh, a mechanism occurs to cause Phase II formation even though atom diffusion is limited, viz., Rh nucleates preferentially and crystallites grow by the addition of Pd (and Rh) atoms which need only diffuse into the Rh kernel to form Phase II ($88 \pm 5\%$ Rh). Hence, the outer shell of the crystallite, Phase I, is in effect, a solid solution deficient in Rh compared with the overall composition. The Rh content of Phase I therefore increases as the Rh flux is increased (Fig. 4).

**Composition range 80–100% Rh.** It is expected that the above mechanism continues but now the composition of the flux is close to the composition of Phase II. Hence it would be difficult, as found, to detect in the diffraction profile the composition difference between the Phase II kernel of the crystallite and the Phase I outer layers which are a little richer in Pd. The catalytic activity for ethylene oxidation over Pd–Rh alloys with compositions in the above ranges is described in (*16*).

## References


1. McKee, D. W., and Norton, F. J., *J. Phys. Chem.* **68**, 481 (1964).
2. McKee, D. W., and Norton, F. J., *J. Catalysis* **4**, 510 (1965).
3. McKee, D. W., and Norton, F. J., *J. Catalysis* **3**, 252 (1964).
4. McKee, D. W., *Trans. Faraday Soc.* **64**, 2200 (1968).
5. Gray, T. J., Masse, N. G., and Oswin, H. G.,

*Actes Congr. Intern. Catalyse, 2e, Paris, 1960* **2,** 1697 (1961).

6. RYLANDER, P. N., AND COHN, G., *Actes Congr. Intern. Catalyse, 2e, Paris, 1960* **1,** 977 (1961).
7. BOND, G. C., AND WEBSTER, D. E., *Platinum Metals Rev.* **9,** 12 (1965).
8. BOND, G. C., AND WEBSTER, D. E., *Platinum Metals Rev.* **10,** 10 (1966).
9. YOSHIDA, K., *J. Chem. Soc. Japan, Pure Chem. Sect.* **88,** 125, 222 (1967).
10. YOSHIDA, K., *Shokubai (Tokyo)* **10,** 2 (1968).
11. SACHTLER, W. M. H., AND DORGELO, G. J. H., *J. Catalysis* **4,** 654 (1965).
12. SACHTLER, W. M. H., AND JONGEPIER, R., *J. Catalysis* **4,** 665 (1965).
13. MOSS, R. L., AND THOMAS, D. H., *J. Catalysis* **8,** 151 (1967).
14. MOSS, R. L., AND THOMAS, D. H., *J. Catalysis* **8,** 162 (1967).
15. MOSS, R. L., AND THOMAS, D. H., *Trans. Faraday Soc.* **60,** 1110 (1964).
16. MOSS, R. L., GIBBENS, H. R., AND THOMAS, D. H., *J. Catalysis* in press.
17. RAUB, E., BEESKOW, H., AND MENZEL, D., *Z. Metallk.* **50,** 428 (1959).
18. MYLES, K. M., *Trans. Met. Soc. AIME* **242,** 1523 (1968).
19. BARTON, J. C., GREEN, J. A. S., AND LEWIS, F. A., *Trans. Faraday Soc.* **62,** 960 (1966).
20. TVERDOVSKII, I. P., AND STETSENKO, A. I., *Dokl. Akad. Nauk. SSSR* **84,** 997 (1952).
21. HOARE, J. P., *J. Electrochem. Soc.* **107,** 820 (1960).
22. NEUGEBAUER, C. A., *in* "Physics of Thin Films" (G. Hass and R. E. Thun, eds.), Vol. 2, p. 1. Academic Press, New York, 1964.